

# A Study on the Effectiveness of Alternative Commercial Ventilation Inlets That Improve Energy Efficiency of Building Ventilation Systems

Brian Considine, Aonghus McNabola, John Gallagher, Prashant Kumar

**Abstract**—Passive air pollution control devices known as aspiration efficiency reducers (AER) have been developed using aspiration efficiency (AE) concepts. Their purpose is to reduce the concentration of particulate matter (PM) drawn into a building air handling unit (AHU) through alterations in the inlet design improving energy consumption. In this paper an examination is conducted into the effect of installing a deflector system around an AER-AHU inlet for both a forward and rear-facing orientations relative to the wind. The results of the study found that these deflectors are an effective passive control method for reducing AE at various ambient wind speeds over a range of microparticles of varying diameter. The deflector system was found to induce a large wake zone at low ambient wind speeds for a rear-facing AER-AHU, resulting in significantly lower AE in comparison to without. As the wind speed increased, both contained a wake zone but have much lower concentration gradients with the deflectors. For the forward-facing models, the deflector system at low ambient wind speed was preferred at higher Stokes numbers but there was negligible difference as the Stokes number decreased. Similarly, there was no significant difference at higher wind speeds across the Stokes number range tested. The results demonstrate that a deflector system is a viable passive control method for the reduction of ventilation energy consumption.

**Keywords**—Aspiration efficiency, energy, particulate matter, ventilation.

## I. INTRODUCTION

EXPOSURE to elevated levels of PM has been identified as a leading cause in respiratory and cardiovascular health problems and mortality. PM exposure occurs in both indoor and outdoor environments and relatively low concentrations can lead to negative health effects [1]. Particle infiltration from the ambient to the indoor environment results in a reduction of the indoor air quality (IAQ) and this can vary depending upon the ambient PM concentration. Particles are transported by mechanical ventilation systems, cracks in the building and through particle resuspension from the ingress/ egress of the building occupants [2]. A study by McCreddin et

al. [3] found that office workers spend > 90% of their time in enclosed environments and 30% within their office space.

The heating, ventilation and air conditioning (HVAC) system of a commercial building is supplied with fresh air by an AHU, typically located on the roof. To maintain an acceptable IAQ, a filtration system is installed within the AHU to prevent the transportation of ambient PM to the indoor environment. A consequence of this passive method for removing the particles from a ventilation system is an increase in the pressure drop. Continuous PM deposition upon the filter leads to an increase in energy consumption as this causes the system resistance to rise until saturation [4]. Therefore, the air filtration system has a significant impact on the fan performance and building energy efficiency.

Filters are graded based upon their effective removal efficiency of coarse, fine and ultrafine particles [5]. The use of a finer filter with higher removal efficiency for fine and ultrafine particles will increase the pressure drop and clog faster but improve IAQ. Similarly, coarser filters will reduce the pressure drop but lead to a decrease in IAQ. Significantly, HVAC systems account for 40% of the total energy consumption of a typical commercial building [6]. Therefore, a passive PM control device that acts as a pre-filter could lead to substantial long-term energy savings and a reduction in PM concentrations within the AHU. The purpose of this paper is to develop a passive PM control system using deflector plates that will lead to the reduction in the AE of an AHU through lower concentrations entering the HVAC system, and consequently lower the building energy consumption.

AER has been designed based upon factors influencing AE. AE is the ratio of particle concentration ( $C$ ) sampled in the orifice inlet to the undisturbed ambient air ( $C_0$ ) [7].

$$AE = \frac{C}{C_0} \times 100 \quad (1)$$

The concept of AE was initially used on the design of personal inhalable aerosol samplers where an efficient sampler has an AE of 100%. Hangal and Wilke found that AE can exceed this value with AE of up to 200% for a thin and thick-walled cylindrical sampler [8]. AE has also been used to investigate the aspiration of particles into the human mouth and nose. A recent study by Tao et al. [9] found AE to be as high as 170% depending on the particle diameter for a moving manikin due to an increase in the particle accumulation at faster walking speeds. Although as the particle diameter

Project is sponsored by the Sustainable Energy Authority of Ireland (SEAI).

Brian Considine is with department of Civil, Structural and Environmental Engineering, Trinity College Dublin, Ireland (corresponding author, phone: +353 (1) 896 3837; e-mail: considib@tcd.ie).

Aonghus McNabola and John Gallagher are with Civil, Structural and Environmental Engineering, Trinity College Dublin, Ireland.

Prashant Kumar is with Global Centre for Clean Air Research, Department of Civil and Environmental Engineering, Faculty of Engineering and Physical Sciences (FEPS), University of Surrey, Guildford GU2 7XH, United Kingdom.

increased AE could be lower than 10%. Variables that effect AE include ambient wind velocity ( $U_\infty$ ), ventilation velocity ( $U_s$ ), orifice size, angle of orifice to oncoming wind, particle size ( $d_p$ ), and the Stokes number (St). Typically, with a thin/thick walled sampler, AE is analysed using a combination of the velocity ratio ( $R$ ) and the Stokes number shown in (2) and (3) respectively.

$$R = \frac{U_s}{U_\infty} \quad (2)$$

$$St = \frac{d_p^2 \rho_p U_\infty}{L_c \mu} \quad (3)$$

where  $\rho_p$  and  $L_c$  are the particle density and characteristic length. Two studies have been conducted on the development of an AER. Both examined the effects upon AE of varying the environmental and building operating conditions for large aspirating systems [10], [11]. McNabola et al. developed a scaled experimental AER prototype for an AHU that incorporated an array of cylindrical blunt nosed inlets [10]. This showed the potential for PM control using AE concepts across a range of wind speeds, flow rates and at different inlet orientations relative to the wind direction. A follow up paper was conducted field testing a full-scale AHU with multiple blunt nosed inlets and a control AHU [11]. The number of inlets for the full-scale AER was designed to maintain a ventilation velocity  $< 1$  m/s. The results indicated that the control AHU reached filter saturation before the AER-AHU. Based upon the pressure drop, this resulted in a 75% increase in filter life or a 14% reduction in energy consumption. This paper will examine the effect upon AE when deflector plates are placed around an AER-AHU inlet. It is proposed that the boundary layer separation caused by the deflectors will lead to lower PM concentrations within the ventilation system through ensuring the particles are diverted away from the AHU inlet. It is expected that this will also lead to a reduced concentration build up within the wake formation in front of the AHU inlet.

## II. MATERIALS & METHODS

### A. Numerical Modelling Set-Up

A 2D numerical model was developed of an AHU to simulate particle laden fluid flow using ANSYS Fluent 18.1. The boundary conditions of the fluid domain are illustrated in Fig. 1 (a). The upstream and downstream distances from the AHU were set to a minimum of  $5H$  and  $10H$  respectively. The height of the domain was set to  $5H$  away from the top of the AHU deflector or roof depending on the model. Wind flow around an AHU is analogous to flow around a bluff body and the fluid domain dimensions are based upon recommendations for wind flow around a building [12].

An array of 25 mm orifices was used to represent the AER-AHU. The array of orifices used was chosen as to build upon findings from previous AER-AHU studies [10], [11]. Models were created both without and with the new deflector plates as shown in Figs. 1 (b) and (c) respectively. The deflector

positioning was varied depending on the orientation of the AHU (i.e. rear-facing or forward facing) to the upstream ambient wind. The ventilation velocity was set to 2.5 m/s based upon maximum AHU flow rates by [11] and ambient wind velocities of 2.5 m/s and 7.5 m/s were tested in order to produce a velocity ratio,  $R$ , of 1 and 3 respectively. A range of particle sizes was tested from 2.5-90  $\mu\text{m}$  diameter, which are represented by their corresponding Stokes number.

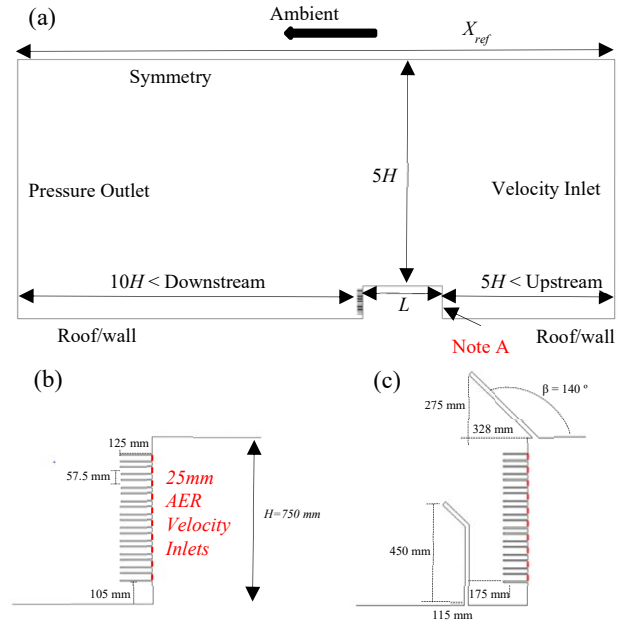


Fig. 1 (a) 2D computational domain for a rear-facing AER-AHU relative to the ambient wind flow. (b) AER-AHU; (c) AER-AHU with deflectors. Note A: Location of AER inlets for forward-facing AHU

An Unsteady Reynolds Averaged Navier-Stokes (URANS) turbulence model is required for a 2D simulation. The  $k-\omega$  SST model due to its effectiveness at modelling both near wall flows and freestream flow in comparison to its standard equivalent and the  $k-\epsilon$  family [13] was employed to simulate fluid flow around the AHU. Numerous studies have used this model to analyze both natural and mechanical ventilation for multi-story buildings [14], [15].

The turbulence model accounts for the fluid flow using an Eulerian reference frame but the pollutant dispersion and trajectory of the microparticles are modelled in a Lagrangian reference frame. This is known as the discrete phase model (DPM) where the particle trajectory is determined by integrating the particle force equation as described in ANSYS Fluent [16]. The particle force equation is dependent upon the drag force of the particle. As the source of the pollutant can vary region to region depending on the local natural or anthropogenic sources, so too will the drag. Therefore, a shape factor is used to model non-spherical particles [17]. To account for the turbulent diffusion and the particle-eddy interaction, the discrete random walk (DRW) model was

chosen as the stochastic tracking method [16].

A transient flow field was used (URANS) with a time step of 0.0005 s and the gradients were assessed with the Green-Gauss node-based method. Second order upwind schemes were chosen for the convective and diffusion terms and a bounded second-order implicit scheme was used for temporal discretization. The pressure-velocity coupling was achieved using SIMPLEC algorithm [18] and the scaled residuals that were set to a minimum of  $10^{-4}$  for all models simulated.

### B. Verification & Validation

The domain was meshed using quadrilaterals cells as these are preferred due to reduced cell count and greater alignment with the fluid flow [19]. A face cell size of 0.05 m was used predominantly throughout the domain along with inflation layers with the first cell height at 0.0001 m, which ensured the appropriate  $Y^+$ . Typically, the CFD process requires that mesh verification is performed as to determine the quality of the model. The grid convergence index (GCI) pioneered by [20] is used extensively to quantify the spatial and temporal discretization error. Verification confirmed that the finest grid which contained approximately 220,000 cells had a  $GCI_{\text{fine}} \leq 3\%$ . Testing occurred at 150-point locations upstream, downstream and around the AHU.

As far as we know no experimental wind tunnel studies currently exist on the AE of an AHU. Validation of the CFD-DPM model was achieved using available experimental wind tunnel results conducted on the AE of a personal aerosol GSP sampler at various particle diameters by [21]. The experimental set up for testing the AE of personal aerosol sampler is comparable to a scaled down version of an AHU test within a wind tunnel. Therefore, the DPM model could be calibrated and validated using this approach. A domain size of 0.1 m x 0.1 m was used where the GSP sampler had an inlet orifice of 0.008 m and a body size of 0.03 m. A global cell size of 0.001 m was used to discretize the domain with a minimum cell height at the walls of 0.0001 m. A suction velocity of 1.16 m/s and ambient wind speed of 0.5 m/s were used as per [21].

The CFD model was in excellent agreement with the experimental wind tunnel results as linear correlation with an  $R^2$  of 0.97 was produced and within the error bar limits as shown in Fig. 2 (a). This is illustrated further in Fig. 2 (b) where the CFD results are typically within the spread of the experimental results with the exception being 58  $\mu\text{m}$  diameter although the deviation is negligible. As the GSP sampler was tested within a low air movement environment and at a low Reynolds number flow, a second validation study was conducted at a higher Reynolds number flow with PM dispersion in an urban environment.

To ensure continuity between the validation models, the boundary conditions, turbulence model and DPM set up were maintained. An isolated urban canyon model was tested at a height (h) and width (w) of 1.6 h giving an aspect ratio of one where  $h = 0.1$  m. An ambient wind speed of 4 m/s and pollutant line source width of 0.7 h was used as per [22]. A cell size of 0.002 m was used for the global grid size and

minimum of 0.0004 m at the walls to ensure  $Y^+$  approximately equal to one. The pollutant concentrations within the canyon were examined through a non-dimensional analysis where  $C_s$  is the pollutant source which is representative of an emission source from a line of cars in traffic. The results demonstrated that the numerical models captured the effects of the actual PM dispersal within a physical environment with an  $R^2$  of 0.95 and similar distribution of PM around the urban canyon as seen in Figs. 3 (a) and (b) respectively.

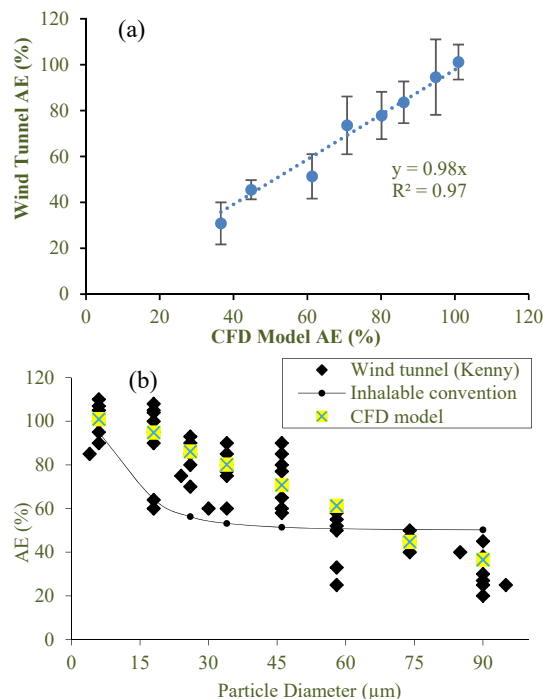


Fig. 2 CFD model comparison against wind tunnel tests on a personal aerosol sampler [21] where (a) Linear correlation between experimental and computational (b) effect of particle diameter on AE

## III. RESULTS & DISCUSSION

### A. Analysis of the AE of an AER-AHU with/without Deflectors at Equivalent Ambient Wind Speed and Ventilation Velocity

An analysis was conducted at varying velocity ratio,  $R$ , to determine the effect on AE for an AER-AHU, both with and without deflectors. The model was tested at both forward and rear-facing orientations (relative to the wind direction) and across their respective range of Stokes numbers, that varied depending on the wind speed and particle diameter. The velocity ratio was chosen based upon previous literature where differing flow dynamics were observed for ambient wind flow around an operating AHU where  $R \leq 1$  and  $R > 1$  [23].

The results in Fig. 4 demonstrate the effectiveness of placing deflectors around the AER-AHU inlet for both AHU orientations at  $R = 1$ . The AE of the forward-facing AER-AHU with deflectors was found to experience lower AE values as the Stokes number increased above one. At  $St < 1$ ,

there is no major difference in AE with or without the deflectors. The rear-facing AHU is also far more effective at reducing the particle concentrations within the ventilation system in comparison to the forward-facing AHU.

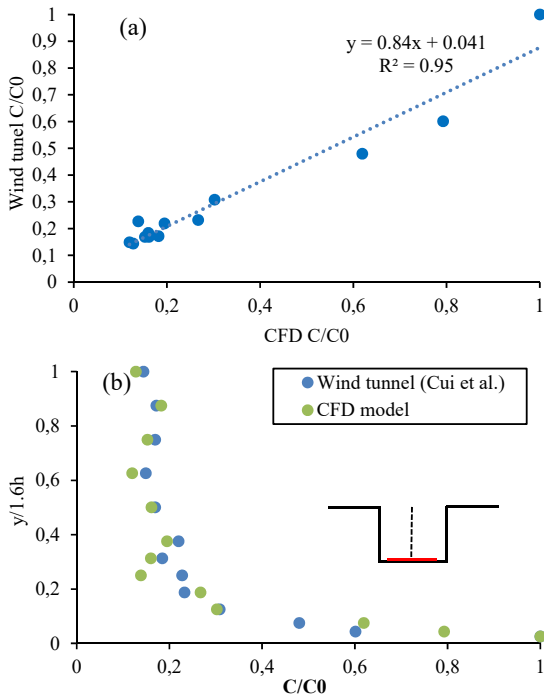


Fig. 3 CFD model of pollutant dispersal within an 2D isolated urban canyon against wind tunnel tests [22] at  $U_{ref}=4m/s$  where (a) Linear correlation between experimental and computational (b) Distribution of PM within the urban canyon

difference in AE with decreasing Stokes numbers with and without deflectors. Where  $2.5 \mu m$  ( $D_{2.5}$ ) and  $10 \mu m$  ( $D_{10}$ ) diameter particles were modelled, there was 18% and 29% difference respectively at their corresponding Stokes numbers. This will result in lower concentrations drawn into the ventilation system at the AHU inlet. This implies significant gains in energy savings from a reduced particle loading upon the filters and lower harmful PM emissions within the indoor environment. As the Stokes number exceeds a magnitude of three the difference in AE is negligible but again significant energy saving will occur up to  $St = 3$ . The rear-facing AER-AHU without deflectors demonstrated similar results for  $D_{2.5}$  AE of 80% at an equivalent ambient wind speed at the original AER-AHU prototype developed and tested by [10].

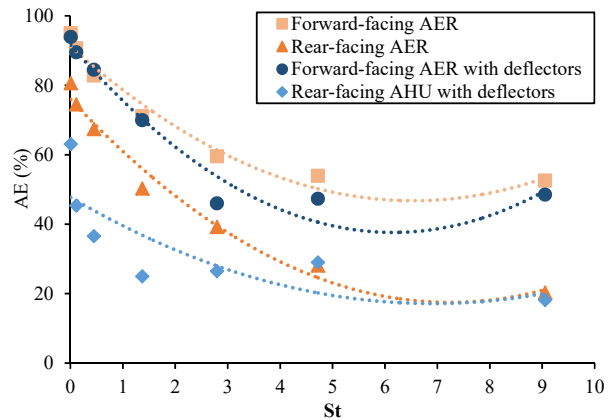


Fig. 4 AE of an AHU-AER with/without deflectors at  $R=1$ , where the ventilation velocity is  $2.5 m/s$

Critically, with the rear-facing AHU there is a considerable

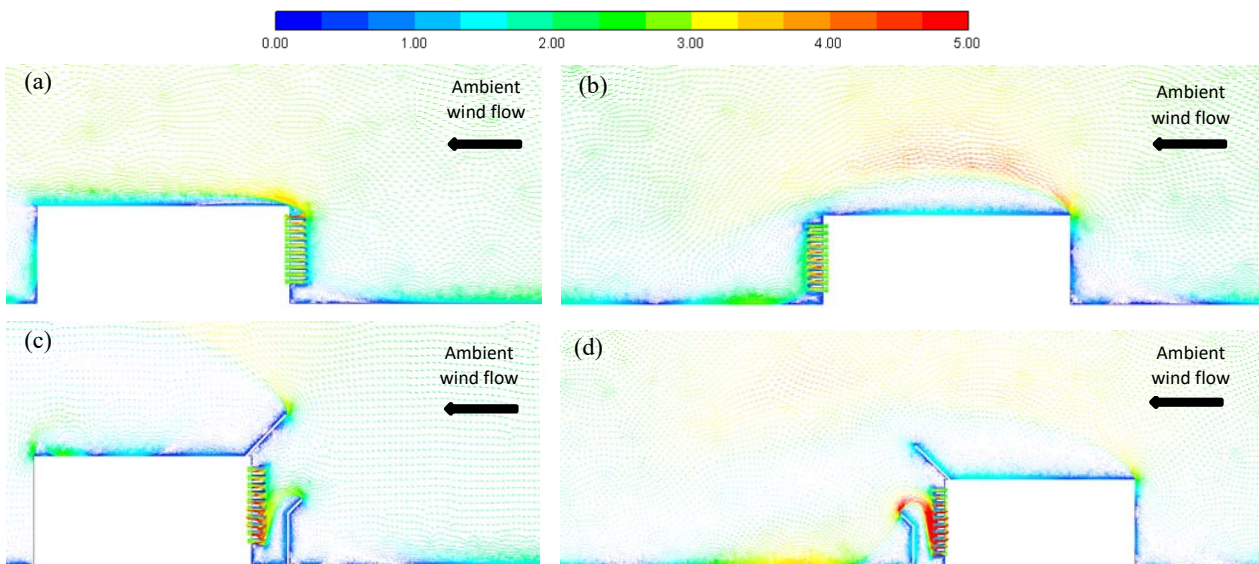


Fig. 5 Velocity vectors (m/s) of ambient wind flow around an AER-AHU at  $R=1$  where (a) forward-facing without deflectors (b) rear-facing without deflectors (c) forward-facing with deflectors (d) rear-facing with deflectors

The variation in AE can be attributed to the change in the aerodynamics around the AER-AHU inlet. The results from velocity vectors of AER-AHU in Figs. 5 (a) and (b) without deflectors are analogous to the study by Considine et al. where similar flow patterns were observed for AHU commercial rainhoods [23]. The ambient wind flow for the forward-facing AER-AHU without deflectors is drawn directly into all ten orifices. For the rear-facing counterpart model, the ambient flow detaches at the back of the AHU and reattaches directly in front of the AHU inlet.

Examining both the forward and rear-facing models with the deflectors in Figs. 5 (c) and (d) shows that they have had a profound impact on the flow dynamics around the AER-AHU inlet. An increase in the magnitude of the velocity can be seen for the lower inlet orifices and a stagnant zone has formed between the upper inlets and the roof deflector. This in combination with the ground deflector has diverted a portion of the flow upwards and around the roof deflector. The most significant difference was detected in the rear-facing AER-AHU with deflectors. The reattachment of the boundary layer has occurred further downstream and consequently the size of the wake zone has increased greatly in front of the AER-AHU.

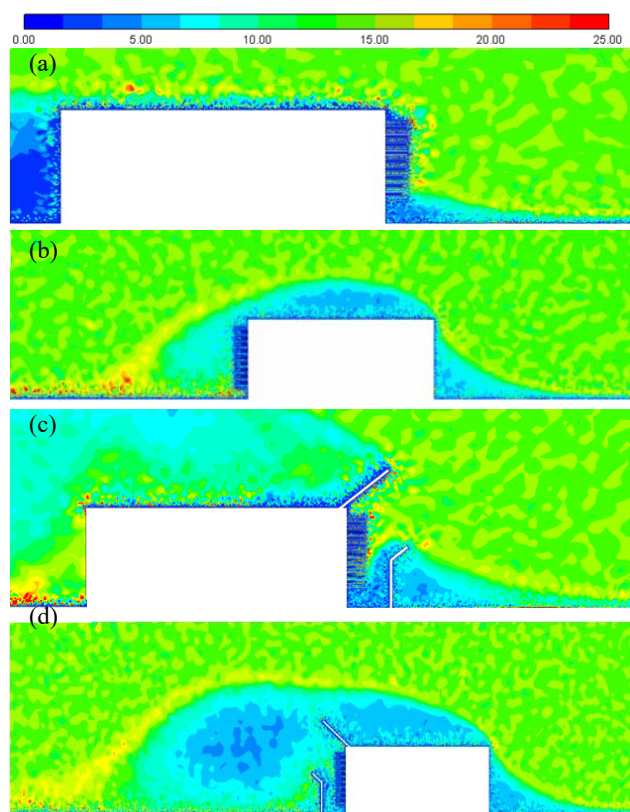


Fig. 6 Contours of  $D_{2.5}$  particle concentrations ( $\mu\text{g}/\text{m}^3$ ) at  $R=1$  where (a) forward-facing without deflectors (b) rear-facing without deflectors (c) forward-facing with deflectors (d) rear-facing with deflectors

The flow similarly to its forward-facing counterpart has split upwards and downwards at the deflectors, although the

flow is not diverted around the AHU but is associated with the eddy formation in front of the ground deflector.

The results from the contours of  $D_{2.5}$  particle concentrations demonstrate the variation in the particle distribution for each model as shown in Figs. 6 (a)-(d). A larger proportion of the orifices in the forward-facing AER-AHU without deflectors were exposed to more ambient PM in comparison to with deflectors. This led to the slight decrease in AE with the deflectors that gradually became larger as the Stokes number increased. A more far-reaching effect of the deflectors can be seen when comparing Figs. 6 (b) and (d).

The large eddy formation and increase in the height of the detached boundary layer has resulted in lower  $D_{2.5}$  particle concentrations around the AHU. The interface between the boundary layer and the freestream flow has also experienced an increased mixing effect resulting in higher concentrations than the ambient environment concentration. This higher concentration is deposited closer to the AHU inlets without deflectors which are then drawn into the orifices. The significant difference in the concentration gradients led to very large difference in AE.

#### *B. Analysis of the AE of an AER-AHU with/without Deflectors at Larger Ambient Wind Speed in Comparison to the Ventilation Velocity*

The ambient wind speed was increased to examine the effect of the deflectors upon the AE of the AER-AHU at  $R = 3$ . The results illustrated in Fig. 7 show that the deflector plates have no major effect on AE for a forward-facing AER-AHU. The trendline shows that the performance of the AER-AHU with and without deflector system are undifferentiated across the Stokes number range examined but can vary at specific individual Stokes number. Inspection of the rear-facing AER-AHU results show similar performance levels at lower Stokes numbers. A 14% and 22% difference in AE occurred for  $D_{2.5}$  and  $D_{10}$  particles respectively with the deflector system compared to without. Again, as the Stokes number becomes larger the deviation in AE between both models is reduced and performance levels are similar. There is not much variation in the velocity vectors at  $R = 3$  for both configurations of the forward-facing AER-AHU in Figs. 8 (a) and (c) in comparison to their equivalent configuration when  $R = 1$

Although the magnitude of the velocity flow field is larger, the stagnant zone underneath the AER inlets without deflectors has increased in size and an equal ventilation velocity for each orifice exists. There has been significant change to the rear-facing AHU without deflectors as a large eddy has now formed in front of the AER-AHU inlet as illustrated in Fig. 8 (b). Similarly, to  $R = 1$  with deflectors and rear-facing, the eddy has formed but increased in size and magnitude as shown in Fig. 8 (d). The results suggest that for both orientations increasing the velocity magnitude generates lower AE for equivalent particle sizes due to difference in magnitude of the Stokes number. For the rear-facing AHU, in combination with the Stokes numbers, the wake effect is also a dominant factor in controlling the trajectory of the

microparticles. The  $D_{2.5}$  particle concentrations showed a similar magnitude to the ambient concentration for the forward-facing AHU without and with deflectors as shown in Figs. 9 (a) and (b) respectively. The bottom three orifices without deflectors are positioned within a wake zone and where the particle concentrations are lower.

Where the deflectors were installed, the bottom orifices also appear to be exposed to lower concentrations in comparison to the upper orifices. Hence, there was no significant difference in AE between both models. The variation between the rear-facing AER-AHU models is evident in the particle concentration gradients within the wake zone for both models. Without the deflectors, there is higher concentration of  $D_{2.5}$  particles in the center of the eddy in comparison to with the deflectors as observed in Fig. 9. This caused the lower AE values in combination with the deflectors directing the particles away from the AER-AHU inlet.

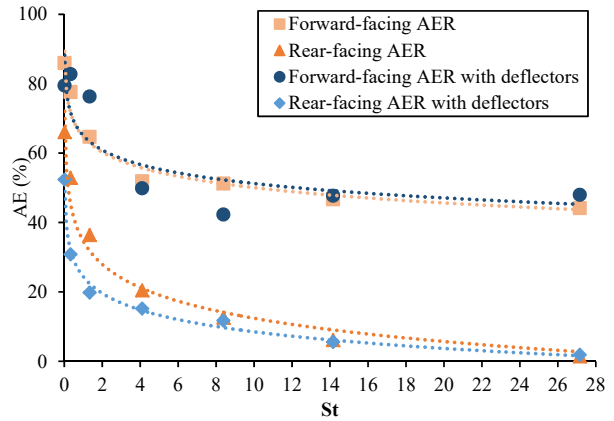


Fig. 7 AE of an AHU-AER with/without deflectors at  $R = 3$ , where the ventilation velocity is 2.5 m/s

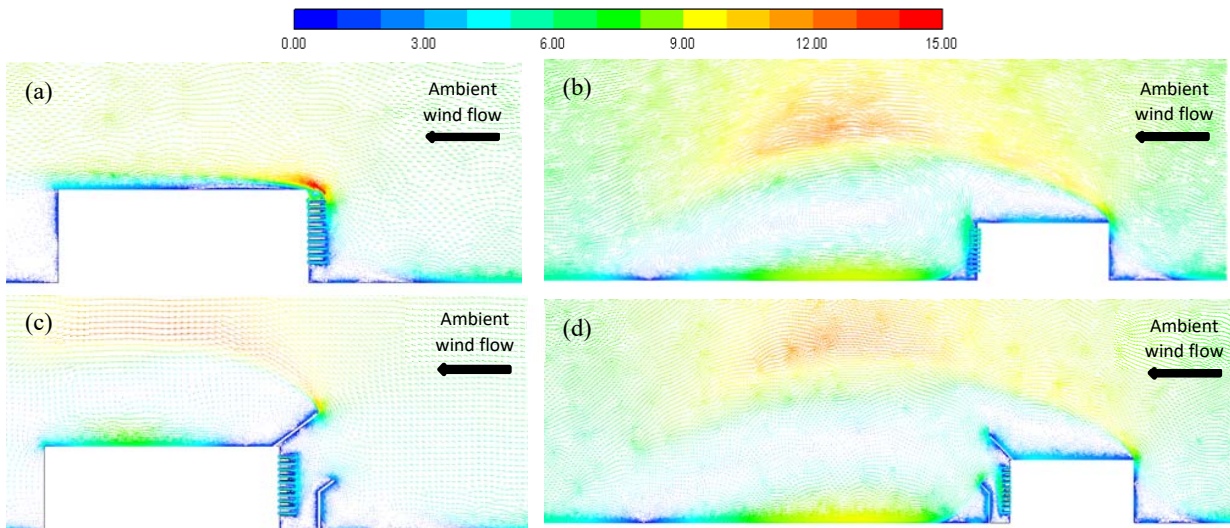


Fig. 8 Velocity vectors (m/s) of ambient wind flow around an AER-AHU at  $R=3$  where (a) forward-facing without deflectors (b) rear-facing without deflectors (c) forward-facing with deflectors (d) rear-facing with deflectors

#### IV. CONCLUSION

The results from this paper demonstrate the potential for deflectors around the AHU inlet as a form of energy efficient pollution control technology for PM. This could lead to significant savings through a reduction in the built environment energy consumption. This paper can be considered a proof of concept and demonstrates that further examination of this technology is warranted. Potential future research will require the following:

1. Parametrized study of the deflectors angle and lengths,
2. Active control system based on wind angle to control orientation,
3. 3D CFD study that includes side deflector,
4. Large eddy simulation (LES) study in place of RANS,
5. Both experimental and field studies to confirm viability of deflectors.

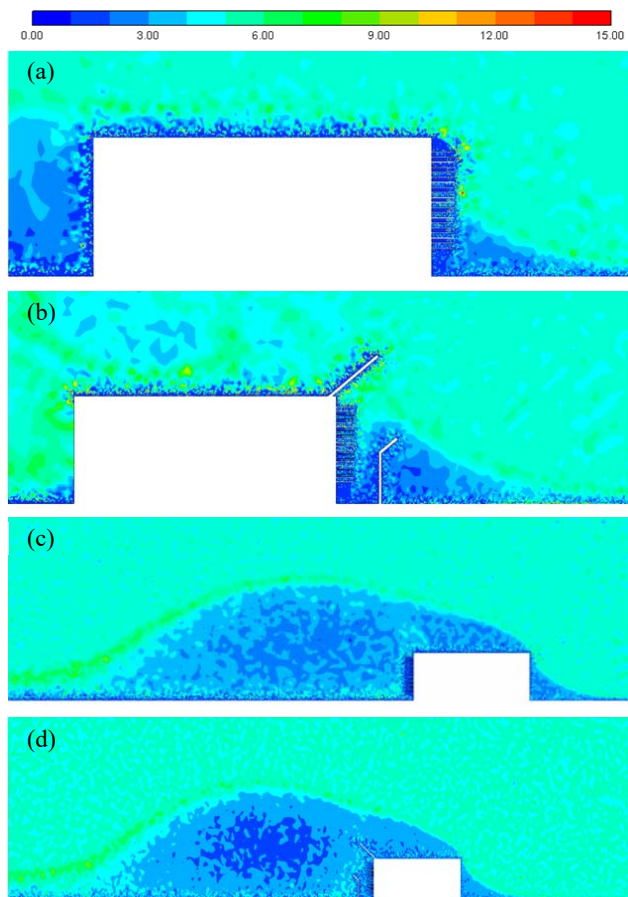


Fig. 9 Contours of  $D_{2.5}$  diameter particle concentrations ( $\mu\text{g}/\text{m}^3$ ) at  $R=3$  where (a) forward-facing without deflectors (b) rear-facing without deflectors (c) forward-facing with deflectors (d) rear-facing with deflectors

#### ACKNOWLEDGMENT

The authors would like to acknowledge that the project has been funded by the Sustainable Energy Authority of Ireland (SEAI), grant number RDD/190. The views and interpretation of this paper are of the authors and do not represent the opinions of the funding source.

#### REFERENCES

- [1] Kim, K.-H., Kabir, E., and Kabir, S., 2015, "A Review on the Human Health Impact of Airborne Particulate Matter," *Environ. Int.*, 74, pp. 136–143.
- [2] Qian, J., Tavakoli, B., Goldasteh, I., Ahmadi, G., and Ferro, A. R., 2014, "Building Removal of Particulate Pollutant Plume during Outdoor Resuspension Event," *Build. Environ.*, 75, pp. 161–169.
- [3] McCreddin, A., Gill, L., Broderick, B., and McNabola, A., 2013, "Personal Exposure to Air Pollution in Office Workers in Ireland: Measurement, Analysis and Implications," *Toxics*, 1, pp. 60–76.
- [4] Feng, Z., Long, Z., and Chen, Q., 2014, "Assessment of Various CFD Models for Predicting Airflow and Pressure Drop through Pleated Filter System," *Build. Environ.*, 75, pp. 132–141.
- [5] ISO 16890-1, 2016, "Air Filters for General Ventilation - Part 1: Technical Specifications, Requirements and Classification System Based upon Particulate Matter Efficiency (EPM) (ISO 16890-1:2016)."
- [6] Yang, Z., Ghahramani, A., and Becerik-Gerber, B., 2016, "Building

- Occupancy Diversity and HVAC (Heating, Ventilation, and Air Conditioning) System Energy Efficiency," *Energy*, 109, pp. 641–649.
- [7] Belyaev, S. P., and Levin, L. M., 1972, "Investigation of Aerosol Aspiration by Photographing Particle Tracks under Flash Illumination," *J. Aerosol Sci.*, 3(2), pp. 127–140.
- [8] Hangal, S., and Willeke, K., 1990, "Aspiration Efficiency: Unified Model for All Forward Sampling Angles," *Environ. Sci. Technol.*, 24(5), pp. 688–691.
- [9] Tao, Y., Yang, W., Inthavong, K., and Tu, J., 2020, "Indoor Particle Inhalability of a Stationary and Moving Manikin," *Build. Environ.*, 169, p. 106545.
- [10] McNabola, A., O'Lunaigh, N., Gallagher, J., and Gill, L., 2013, "The Development and Assessment of an Aspiration Efficiency Reducing System of Air Pollution Control for Particulate Matter in Building Ventilation Systems," *Energy Build.*, 61, pp. 177–184.
- [11] Morgan, D. T., Daly, T., Gallagher, J., and McNabola, A., 2017, "Reducing Energy Consumption and Increasing Filter Life in HVAC Systems Using an Aspiration Efficiency Reducer: Long-Term Performance Assessment at Full-Scale," *J. Build. Eng.*, 12, pp. 267–274.
- [12] Tominaga, Y., Mochida, A., Yoshie, R., Kataoka, H., Nozu, T., Yoshikawa, M., and Shirasawa, T., 2008, "AIJ Guidelines for Practical Applications of CFD to Pedestrian Wind Environment around Buildings," *J. Wind Eng. Ind. Aerodyn.*, 96(10), pp. 1749–1761.
- [13] Menter, F. R., 1994, "Two-Equation Eddy-Viscosity Turbulence Models for Engineering Applications," *AIAA J.*, 32(8), pp. 1598–1605.
- [14] Zhong, H.-Y., Jing, Y., Liu, Y., Zhao, F.-Y., Liu, D., and Li, Y., 2019, "CFD Simulation of 'Pumping' Flow Mechanism of an Urban Building Affected by an Upstream Building in High Reynolds Flows," *Energy Build.*, 202, p. 109330.
- [15] Ramponi, R., and Blocken, B., 2012, "CFD Simulation of Cross-Ventilation for a Generic Isolated Building: Impact of Computational Parameters," *Build. Environ.*, 53, pp. 34–48.
- [16] Fluent Inc., 2018, *ANSYS Fluent Theory Guide*, ANSYS, ANSYS, Inc., 275 Technology Drive Canonsburg, PA 15317.
- [17] Haider, A., and Levenspiel, O., 1989, "Drag Coefficient and Terminal Velocity of Spherical and Nonspherical Particles," *Powder Technol.*, 58(1), pp. 63–70.
- [18] Liu, J., and Niu, J., 2016, "CFD Simulation of the Wind Environment around an Isolated High-Rise Building: An Evaluation of SRANS, LES and DES Models," *Build. Environ.*, 96, pp. 91–106.
- [19] Fluent Inc., 2018, *ANSYS Fluent User Guide*, ANSYS, ANSYS, Inc., 275 Technology Drive Canonsburg, PA 15317.
- [20] Roache, P. J., 1994, "Perspective: A Method for Uniform Reporting of Grid Refinement Studies," *J. Fluids Eng.*, 116(3), pp. 405–413.
- [21] Kenny, L. C., Aitken, R. J., Baldwin, P. E. J., Beaumont, G. C., and Maynard, A. D., 1999, "The Sampling Efficiency of Personal Inhalable Aerosol Samplers in Low Air Movement Environments," *J. Aerosol Sci.*, 30(5), pp. 627–638.
- [22] Cui, P.-Y., Li, Z., and Tao, W.-Q., 2017, "Numerical Investigations on Re-Independence for the Turbulent Flow and Pollutant Dispersion under the Urban Boundary Layer with Some Experimental Validations," *Int. J. Heat Mass Transf.*, 106, pp. 422–436.
- [23] Considine, B., McNabola, A., Kumar, P., and Gallagher, J., "Numerical Analysis of the Particle Aspiration Efficiency for a Building Ventilation System under Various Physical and Environmental Operating Conditions," *J. Environ. Manage.*, submitted for publication.